



## Short Communication

## Highly transparent RF magnetron-sputtered indium tin oxide films for a-Si:H/c-Si heterojunction solar cells amorphous/crystalline silicon



Shahzada Qamar Hussain<sup>a,b</sup>, Woong-Kyo Oh<sup>c</sup>, Shihyun Ahn<sup>c</sup>, Anh Huy Tuan Le<sup>c</sup>, Sunbo Kim<sup>a</sup>, S.M. Iftiqar<sup>c</sup>, Subramaniam Velumani<sup>c,d</sup>, Youngseok Lee<sup>a</sup>, Junsin Yi<sup>a,c,\*</sup>

<sup>a</sup> Department of Energy Science, Sungkyunkwan University, Suwon 440-746, Republic of Korea

<sup>b</sup> Department of Physics, COMSATS Institute of Information and Technology, Lahore 54000, Pakistan

<sup>c</sup> College of Information and Communication Engineering, Sungkyunkwan University, Suwon 440-746, Republic of Korea

<sup>d</sup> Department of Electrical Engineering-SEES, CINVESTAV-IPN, Col San Pedro Zacatenco, D.F., Mexico C.P 07360, Mexico

## ARTICLE INFO

Available online 13 April 2014

## Keywords:

ITO films

RF power

Carrier lifetime

Anti-reflection electrode

amorphous/crystalline silicon

## ABSTRACT

We prepared highly transparent magnetron-sputtered indium tin oxide (ITO) films deposited at various RF powers for a-Si:H(p)/c-Si heterojunction solar cell applications. The surface morphology of ITO films improved in terms of an increase in grain size as the RF power increased. Rapid growth of the (400) plane was observed with increasing RF power, while the (222) plane remain unchanged. The ITO film deposited at 100 W showed the lowest resistivity of  $3.8 \times 10^{-4} \Omega \text{ cm}$  and highest visible transmittance of 90.19%. The deposition rate and optical bandgap of ITO films were varied from 20 to 100 nm/min and from 3.68 to 3.77 eV for RF power from 50 to 250 W, respectively. Highly transparent ITO films were utilized as the front anti-reflection layer in heterojunctions with intrinsic thin-layer (HIT) solar cells showed the efficiency of 16.3% for RF power of 100 W. The HIT solar cells deposited at RF power of 100 W also exhibited higher carrier lifetime and implied voltage.

© 2014 Elsevier Ltd. All rights reserved.

## 1. Introduction

Solar energy is a renewable energy resource but it is necessary to improve the performance and decrease the cost to use solar cells as alternative energy resources. Heterojunction with intrinsic thin-layer (HIT) solar cells have emerged as high-efficiency devices that use hydrogenated amorphous silicon (a-Si:H) and crystalline silicon

(c-Si) technologies. HIT solar cells are renowned for their low cost, low deposition temperature, high efficiency and good stability [1,2].

Transparent conductive oxide (TCO) films are used as anti-reflection electrodes in most optoelectronic devices such as flat panel displays and solar cell applications. Various types of TCO films such as Al-doped zinc oxide (AZO), Ga-doped zinc oxide and indium tin oxide (ITO) are under ongoing investigation owing to their low resistivity and high transparency [3–5]. ITO films are preferred as TCO materials because of their high conductivity, visible transmittance and wide optical bandgap for optoelectronic applications. ITO films can be deposited via various techniques including spray pyrolysis, sol–gel methods, atomic

\* Corresponding author at: Sungkyunkwan University, College of Information and Communication Engineering, 300, Cheoncheon-dong, Jangan-gu, Suwon, Gyeonggi-do, 440-746 Korea, Republic of Korea. Tel.: +82 31 290 7139; fax: +82 31 290 7159.

E-mail addresses: [yi@yurim.skku.ac.kr](mailto:yi@yurim.skku.ac.kr), [sqamar@skku.edu](mailto:sqamar@skku.edu) (J. Yi).

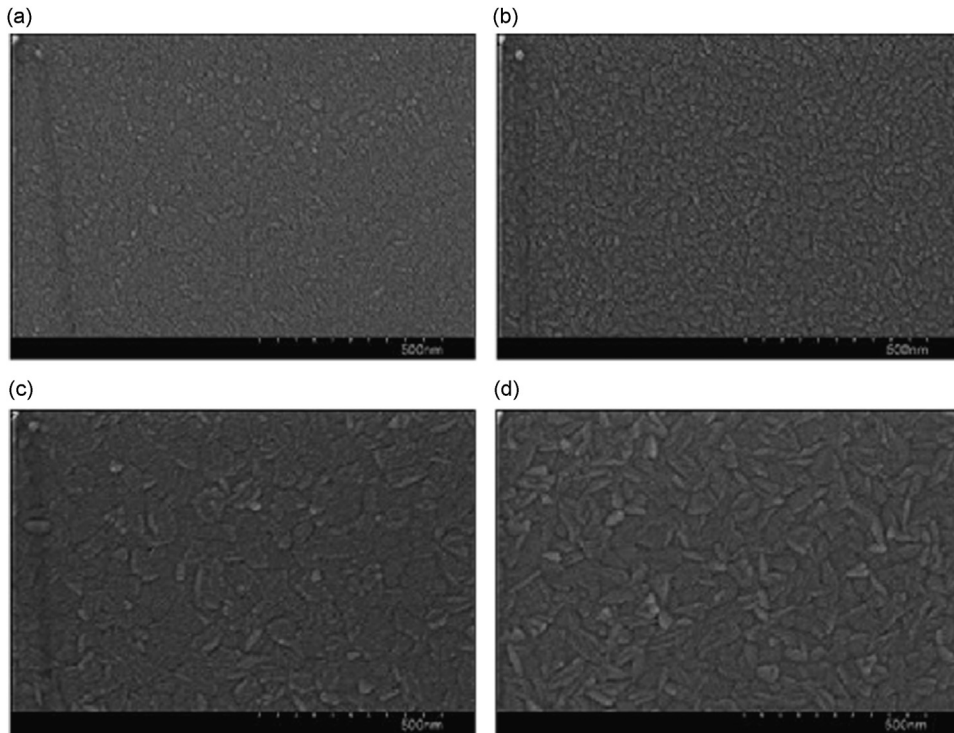


Fig. 1. SEM images of ITO films for RF power of (a) 50 W, (b) 100 W, (c) 200 W, and (d) 250 W.

layer deposition, chemical vapor deposition (CVD), pulsed laser deposition and magnetron sputtering [5–10]. Magnetron sputtering is preferred as it yields the films with superior electrical and optical properties and good surface uniformity and adherence. Radio-frequency (RF) magnetron sputtering is an efficient method because the film properties can be controlled by varying the sputtering parameters such as substrate temperature [11,12,27], working pressure [13], film thickness [14], RF power [15,16] and  $O_2$  flow rate [5,17]. The substrate temperature and RF power are the most critical process parameters since they influence the film quality and material properties such as the electrical, optical and surface behavior. The influence of RF power on the electrical, optical, and structural properties of AZO films was investigated by Kuo et al. and Rahmane et al. [18,19]. Nisha et al. and Vidhya et al. found that the electrical, optical and surface characteristics of ITO films can be improved by RF power [15,20]. Even though there have been several studies on the influence of RF power on the electrical, optical and structural properties of magnetron-sputtered ITO films, the influence of highly transparent ITO films deposited at various RF powers on HIT solar cells has rarely been reported.

In this study we investigated the influence of RF power on magnetron-sputtered ITO films for a-Si:H/c-Si heterojunction solar cells. The electrical and optical characteristics of the ITO films as a function of RF power are described, as well as their surface morphology and structural properties. The influence of RF power on HIT solar cell performance and the effect of carrier lifetime on the implied voltage are discussed.

## 2. Experimental details

Glass substrates (Corning Eagle) were used for the deposition of ITO films by RF magnetron sputtering system. The sputter ITO target was composed of 90 wt.%  $In_2O_3$  and 10 wt.%  $SnO_2$  with 99.999% purity. The base pressure of the chamber was fixed to  $9 \times 10^{-5}$  Torr and the working pressure was  $1.5 \times 10^{-3}$  Torr. The substrate temperature was kept constant at 200 °C while the Ar flow rate was maintained at 20 sccm. The RF power was varied from 50 to 250 W during the sputtering process. A schematic diagram of a-Si:H/c-Si heterojunction solar cell can be found elsewhere [5]. Monocrystalline n-type Si wafers (525  $\mu$ m, 1–10  $\Omega$  cm) were used as the base material for the preparation of HIT solar cells. Standard RCA 1 ( $H_2O_2$ – $NH_4OH$ – $H_2O$ ) and RCA 2 ( $H_2O_2$ – $HCl$ – $H_2O$ ) processes were used to clean the wafers after an ultrasonic treatment. Plasma-enhanced chemical vapor deposition (PECVD) was used to deposit a-Si:H(p/i) layers of 7 and 5 nm in thickness on the front side of a c-Si wafer. The a-Si:H(i/n) layers with the thickness of 5 and 7 nm were deposited on the rear side of the c-Si wafer. The 100-nm ITO films were deposited on the front side of the HIT solar cell using a metal mask placed directly on the a-Si:H(p)-coated surface. Finally, thermal evaporation was used to deposit Ag/Al and Al electrodes on the front and rear surfaces for good ohmic contacts. The active area of the HIT solar cell was fixed to  $0.6 \times 0.6$  cm<sup>2</sup>.

The ITO film thickness was measured spectroscopically (Nano-view, SE MF-1000) at room temperature. The surface morphology of films was observed by scanning electron microscopy (SEM; Hitachi S-4800). The electrical

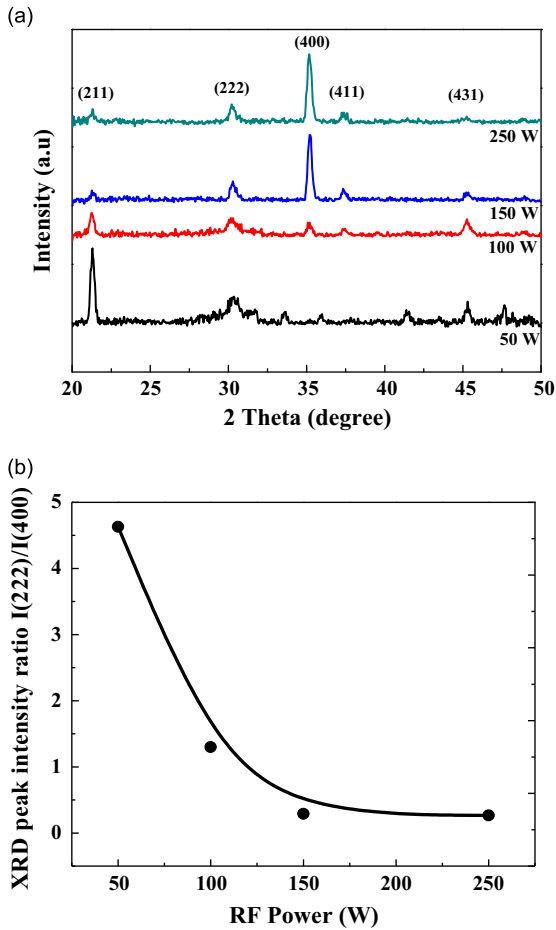


Fig. 2. (a) XRD patterns and (b) XRD peak intensity ratio  $I(222)/I(400)$  for ITO films as a function of RF power.

characteristics like resistivity, carrier concentration and Hall mobility were determined by Hall effect measurement system (Ecopia HMS-3000). The optical transmittance of ITO films was measured by UV-Vis spectrophotometer (SCINCO S-3100) at room temperature. The structural properties of ITO films were analyzed by X-ray diffraction (XRD; Panalytical PW 3060) using  $\text{Cu K}\alpha$  radiation (0.1541 nm). The performance of HIT solar cells was characterized by measuring the current density–voltage (J–V) characteristics under AM 1.5 and  $100 \text{ mW/cm}^2$  at room temperature. The effective carrier lifetime of HIT solar cells with and without an ITO layer was determined in terms of the quasi-steady-state photoconductance using a WCT-120 lifetime measurement system (Sinton Consulting).

### 3. Results and discussion

Fig. 1(a–d) shows the SEM images of ITO films for various RF powers. The film deposited at 50 W was smooth and amorphous because of insufficient thermal energy. When the RF power was increased from 50 to 100 W, a random crystallographic orientation was observed on the substrate. The surface grain size of ITO films gradually

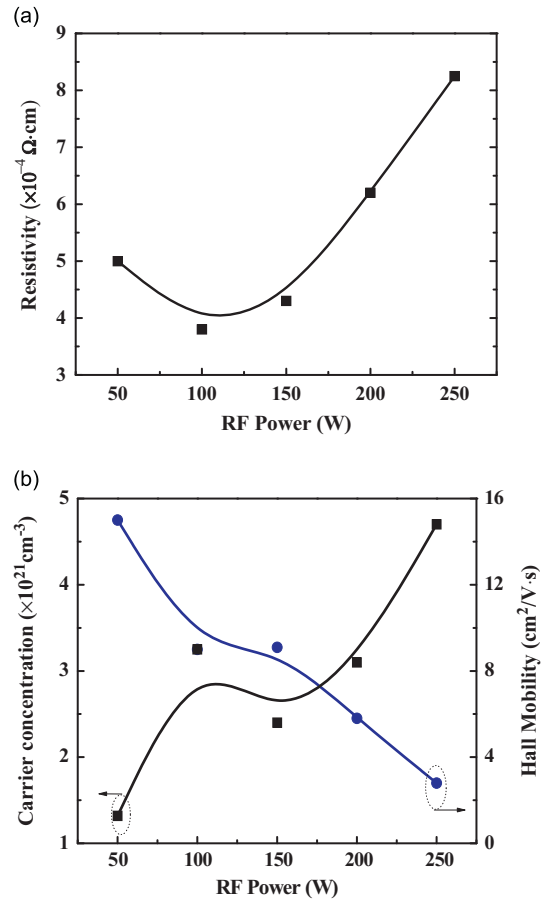


Fig. 3. (a) Resistivity, (b) Hall mobility and carrier concentration of ITO films for various RF powers.

increased with RF power. The maximum grain size was observed by the film deposited at 250 W. Higher RF power led to higher adatom energy during sputtering and resulted in a larger grain size on the film surface [19,21].

Fig. 2(a) shows the XRD patterns for ITO films for various RF powers. All the films except that prepared at 50 W were polycrystalline and exhibit various diffraction peaks. The crystallinity of the films improved with increasing RF power. An increase of RF power had no effect on the (222) diffraction peak. As the RF power was increased beyond 50 W, a (400) diffraction peak was observed at  $2\theta = 35^\circ$  corresponding to  $\text{In}_2\text{O}_3$  with a preferred [100] orientation. There was a large increase in the (400) peak intensity above 100 W. This was ascribed to an increased  $\text{O}_2$  removal phenomenon due to the increase of RF power [18,19]. The XRD intensity ratio  $I(222)/I(400)$  for the ITO films is shown in Fig. 2(b). For the RF power of 50 W, the  $I(222)/I(400)$  ratio was 4.63. This ratio decreased from 1.3 to 0.266 as the RF power was increased from 100 to 250 W. For ITO films sputtered in pure argon, the preferential orientation along the [100] direction was always more pronounced at higher RF power [22]. Higher RF power increases the mobile energy of sputtered atoms on substrates and hence improves the crystallinity of ITO films.

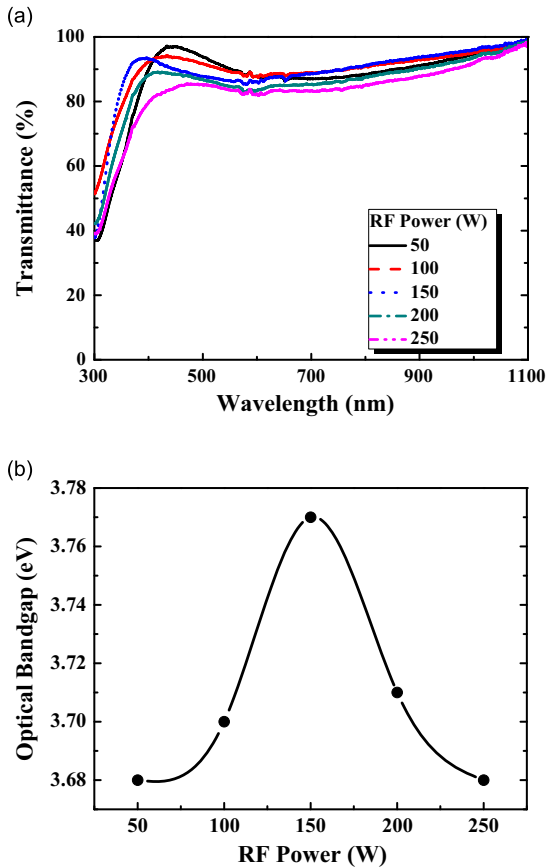


Fig. 4. (a) Transmittance and (b) optical bandgap of ITO films for various RF powers.

Fig. 3(a,b) shows the electrical characteristics (resistivity, Hall mobility, and carrier concentration) of ITO films prepared at various RF powers. The resistivity of ITO films was decreased from  $5 \times 10^{-4}$  to  $3.8 \times 10^{-4} \Omega \cdot \text{cm}$  when the RF power increased from 50 to 100 W. As the RF power increased from 150 to 250 W, the film resistivity increased from  $4.3 \times 10^{-4}$  to  $8.25 \times 10^{-4} \Omega \cdot \text{cm}$ . The decrease in resistivity with increasing RF power was related to film crystallinity or to deviation from stoichiometry, while the increase in resistivity can be attributed to the high-energy bombardment effects of argon ions in the plasma [23]. The improvement in resistivity of ITO films may also be related to higher number of free carriers with increasing RF power. The Hall mobility of the ITO films gradually decreased from 15 to  $2.8 \text{ cm}^2/\text{V} \cdot \text{s}$  while carrier concentration increased from  $1.32 \times 10^{21}$  to  $4.7 \times 10^{21} \text{ cm}^{-3}$  as the RF power increased from 50 to 250 W. The increase in carrier concentration was related to an increase in oxygen vacancies and  $\text{Sn}^{4+}$  concentration, as evident from the appearance of a (400) diffraction peak in the XRD patterns with increasing RF power.

The optical transmittance of ITO films prepared at various RF powers is shown in Fig. 4(a). All the ITO films were highly transparent in the visible (400–800 nm) wavelength region and showed average transmittance of

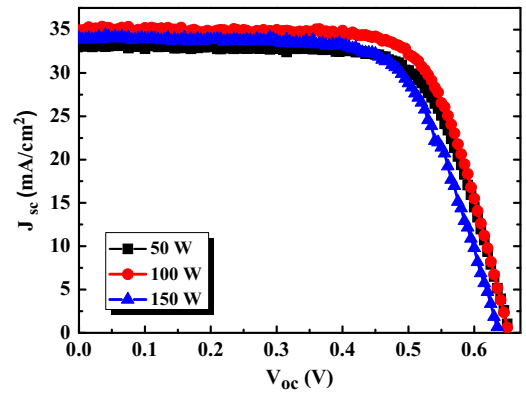


Fig. 5. The current density–voltage (J–V) characteristics of HIT solar cells for various RF powers.

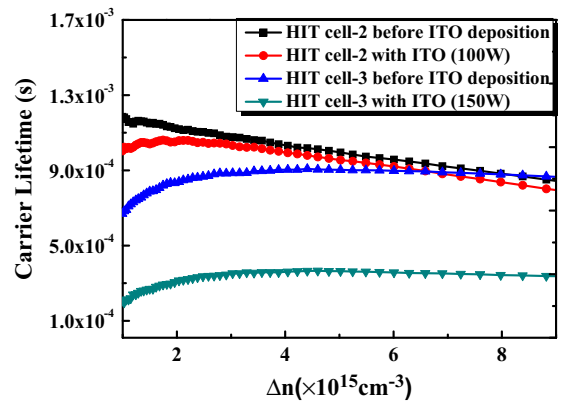


Fig. 6. Carrier lifetime for HIT solar cell as a function of the minority carrier density before and after deposition of ITO films for various RF powers.

above 85%. For the film prepared at 50 W, the average visible transmittance was 90.14%. The transmittance decreased from 90.19% to 83.61% as the RF power increased from 100 to 250 W. The maximum visible transmittance (90.19%) was observed for ITO films prepared at 100 W. The ITO films showed even higher transmittance in the visible–near infra-red (Vis–NIR) wavelength (400–1100 nm) region. There was a decrease in transmittance at higher wavelengths with increasing RF power that may be related to free carrier absorption. An increase of carrier concentration for the ITO films resulted in an increase in free carrier absorption. Nisha et al. reported that an increase in carrier concentration with RF power led to reflection of incident wavelength in the infra-red (IR) region by TCO films [15].

Fig. 4(b) shows the optical bandgap of ITO films for various RF powers. The direct transition model was used to obtain the optical bandgap from plot of photon energy ( $h\nu$ ) versus  $(\alpha h\nu)^2$ . The absorption coefficient  $\alpha$  was determined from the relation  $\alpha = (1/d) \ln(1/T)$ , where  $d$  is the film thickness and  $T$  being the transmittance. The optical bandgap of ITO films increased from 3.68 to 3.77 eV as the RF power was increased from 50 to 150 W. As the RF power was further increased from 150 to 250 W, the optical bandgap of films decreased from 3.77 to 3.678 eV.

**Table 1**  
Performance of HIT solar cells for various RF powers.

RF power (W)	$V_{oc}$ (mV)	$J_{sc}$ (mA/cm <sup>2</sup> )	FF (%)	Efficiency (%)
50	650	33.1	70.43	15.2
100	650	34.91	71.6	16.3
150	635	34.0	68.4	14.8

**Table 2**  
Effective carrier lifetime and implied voltage ( $V_{oc}$ ) for HIT solar cells before and after ITO film deposition for various RF powers.

	Carrier lifetime ( $\mu$ s)	$V_{oc}$ (mV)
HIT solar cell-2 before ITO deposition	1126	672
HIT solar cell-2 with ITO (100 W)	1053	670
HIT solar cell-3 before ITO deposition	880	665
HIT solar cell-3 with ITO (150 W)	362	628

Widening of optical bandgap was related to the Burstein–Moss effect, while narrowing of optical bandgap can be attributed to electron–electron and electron–impurity scattering due to higher carrier concentration [5,15,16].

Fig. 5 shows the current density–voltage (J–V) characteristics for HIT solar cells prepared at various RF powers. The HIT solar cell prepared at 50 W showed a short-circuit current density ( $J_{sc}$ ) of 33.1 mA/cm<sup>2</sup>, a fill factor (FF) of 70.43%, and an open-circuit voltage ( $V_{oc}$ ) of 650 mV. The  $J_{sc}$  increased from 33.1 to 34.91 mA/cm<sup>2</sup> and FF from 70.43% to 71.6% as the RF power was increased from 50 to 100 W. The increase in  $J_{sc}$  was related to the resistivity, transmittance, optical bandgap and crystallinity of the ITO films. As the RF power was further increased from 100 to 150 W, there was a decrease in  $J_{sc}$  from 34.91 to 34.0 mA/cm<sup>2</sup>, FF from 71.6% to 68.4%, and  $V_{oc}$  from 650 to 635 mV for the HIT solar cells (Table 1). The variations in  $V_{oc}$  and FF for the HIT solar cells mainly depend on the resistivity, crystallinity and work function of the ITO films [5,24]. The maximum HIT solar cell performance was shown to be;  $J_{sc} = 34.91$  mA/cm<sup>2</sup>,  $V_{oc} = 650$  mV, FF = 71.6%, and  $\eta = 16.3\%$  for RF power of 100 W.

Fig. 6 shows the carrier lifetime of HIT solar cells as a function of minority carrier density for various RF powers. The excess carrier lifetime is a measure of how long a generated carrier remains in an excited state. Therefore, higher carrier lifetimes are preferred for high implied voltage ( $V_{oc}$ ) [25,26]. The HIT solar cells with and without an ITO layer had a carrier lifetime of 1053 and 1126  $\mu$ s, respectively, for RF power of 100 W. The HIT solar cell deposited at 150 W had a low carrier lifetime of 362 and 880  $\mu$ s with and without an ITO layer, respectively. The carrier lifetime influences  $V_{oc}$  of HIT solar cell, as reported by Taguchi et al [26]. The HIT solar cell deposited at 100 W had  $V_{oc}$  of 670 and 672 mV with and without ITO layers, respectively (Table 2).

## 4. Conclusion

In summary, magnetron-sputtered ITO films with low resistivity of  $3.8 \times 10^{-4} \Omega$  cm and high visible transmittance of 92% were deposited at various RF powers. An increase in RF power influenced the surface grain size of ITO films and the crystallinity improved along the (400) orientation. Higher RF power resulted in a decrease of ITO film conductivity was related to high-energy bombardment effects of argon ions in the plasma. The decrease in optical transmittance at higher RF power was due to free carrier absorption resulted from an increase in carrier concentration. The change in optical bandgap for ITO films was due to the Burstein–Moss effect and electron–electron and electron–impurity scattering. The highly transparent ITO films were used as the front anti-reflection layer in HIT solar cells. The best photovoltaic parameters were observed to be;  $V_{oc} = 650$  mV,  $J_{sc} = 34.91$  mA/cm<sup>2</sup>, FF = 71.6%, and  $\eta = 16.3\%$  for RF power of 100 W. The HIT solar cell deposited at 100 W had an implied voltage of 710 and 712 mV with and without ITO layer, respectively.

## Acknowledgments

This work was supported by the Human Resources Development program (No. 20124010203280) of the Korea Institute of Energy Technology Evaluation and Planning (KETEP) grant funded by the Korea government Ministry of Trade, Industry and Energy.

## References

- [1] V.A. Dao, J. Heo, H. Choi, J. Yi, Sol. Energy 84 (2010) 777–783.
- [2] N.H. Como, A.M. Acevedo, Sol. Energy Mater. Sol. Cells 94 (2010) 62–67.
- [3] F. Wang, M.Z. Wu, Y.Y. Wang, Y.M. Yu, X.M. Wu, L.J. Zhuge, Vacuum 89 (2013) 127–131.
- [4] I. Shakir, M. Shahid, M. Nadeem, D.J. Kang, Electrochim. Acta 72 (2012) 134–137.
- [5] S.Q. Hussain, W.K. Oh, S. Ahn, A.H.T. Le, S. Kim, Y. Lee, J. Yi, Vacuum 101 (2014) 18–21.
- [6] S.M. Rozati, T. Ganj, Renew. Energy 29 (2004) 1671–1676.
- [7] M.J. Alam, D.C. Cameron, Thin Solid Films 377–378 (2000) 455–459.
- [8] S.T. Hwang, C.B. Park, Trans. Electr. Electron. Mater. 11 (2010) 81–84.
- [9] I. Shakir, M. Shahid, D.J. Kang, Chem. Commun. 46 (2010) 4324–4326.
- [10] C. Viespe, I. Nicolae, C. Sima, C. Grigoriu, R. Medianu, Thin Solid Films 515 (2007) 8771–8775.
- [11] V. Ai Dao, H. Choi, J. Heo, J. Yi, Curr. Appl. Phys. 10 (2010) S506–S509.
- [12] W.K. Oh, S.Q. Hussain, Y.J. Lee, Y. Lee, S. Ahn, J. Yi, Mater. Res. Bull. 47 (2012) 3032–3035.
- [13] R. Das, K. Adhikary, S. Ray, Appl. Surf. Sci. 253 (2007) 6068–6073.
- [14] K. Jagadeesh Kumar, N. Ravi Chandra Raju, A. Subrahmanyam, Appl. Surf. Sci. 257 (2011) 3075–3080.
- [15] M. Nisha, M.K. Jayaraj, Appl. Surf. Sci. 255 (2008) 1790–1795.
- [16] C.N.D. Carvalho, A. Luis, O. Conde, E. Fortunato, G. Lavareda, A. Amaral, J. Non-Cryst. Solids 299–302 (2002) 1208–1212.
- [17] Y.L. Lee, K.M. Lee, Trans. Electr. Electron. Mater. 10 (2009) 203–207.
- [18] S.Y. Kuo, K.C. Liu, F.I. Lai, J.F. Yang, W.C. Chen, M.Y. Hsieh, H.I. Lin, W.T. Lin, Microelectron. Reliab. 50 (2010) 730–733.
- [19] S. Rahmane, M.A. Djouadi, M.S. Aida, N. Barreau, B. Abdallah, N. Hadj Zoubir, Thin Solid Films 519 (2010) 5–10.
- [20] V.S. Vidhya, V. Malathy, T. Balasubramanian, V. Saaminathan, C. Sanjeeviraja, M. Jayachandran, Curr. Appl. Phys. 11 (2011) 286–294.
- [21] L.M. Shui, P.Z. Yong, X.X. Wu, D. Ying, H.S. Hao, Chin. Phys. 16 (2007) 548–552.
- [22] E. Terzini, P. Thilakan, C. Minarini, Mater. Sci. Eng. B 77 (2000) 110–114.

- [23] M. Saad, A. Kassis, *Mater. Chem. Phys.* **136** (2012) 205–209.
- [24] S.Q. Hussain, S. Kim, S. Ahn, N. Balaji, Y. Lee, J.H. Lee, J. Yi, *Sol. Energy Mater. Sol. Cells* **122** (2014) 130–135.
- [25] L. Fesquet, S. Olibet, J.D. Lacoste, S.D. Wolf, A.H. Wyser, C. Monachorr, C. Ballif, in: Proceedings of the 34th IEEE Photovoltaic Specialists Conference, 2009, pp. 754–758.
- [26] M. Taguchi, H. Sakata, Y. Yoshimine, E. Maruyama, A. Terakawa, M. Tanaka, S. Kiyama, in: Proceedings of the 31st IEEE Photovoltaic Specialists Conference, 2005, pp. 866–871.
- [27] S. Cho, *Trans. Electr. Electron. Mater.* **10** (2009) 185–188.